AUTOMATIC DETECTION OF SUB-KILOMETER CRATERS IN HIGH RESOLUTION IMAGES OF MARS. Erik R. Urbach, *Lunar and Planetary Institute, Houston TX 77058-1113, USA, (urbach@lpi.usra.edu)*, Tomasz F. Stepinski, *Lunar and Planetary Institute, Houston TX 77058-1113, USA, (tom@lpi.usra.edu).*

Introduction. A new method for automatic detection of sub-km impact craters in high resolution images of Mars is presented. This new method complements our earlier work [1] that focused on detecting larger (diameter > 3 km) craters from Mars Orbiter Laser Altimeter (MOLA) topography. Due to limited resolution of topography data, smaller craters must be detected from images. In addition, craters-from-images approach has application for other planetary bodies where topographic data is not available.

The purpose of the present method is to find craters in high resolution images. This contribution focuses on images from the High Resolution Stereo Camera (HRSC) instrument of the MarsExpress orbiter. We use nadir panchromatic HRSC images having resolution of up to 12.5 m/pixel. In such images, the smallest craters one can expect to detect have diameters of 10 pixels or about 125 m. On the other hand, large craters on Mars have already been cataloged, either manually e.g., Barlow [2], or automatically from topography (our work in progress). Therefore, our method is designed to detect craters with diameters ranging between 125 m and 5 km.

A common approach to locate craters in images is to use edge detection techniques. However, these existing methods are unable to detect smaller craters. Our approach, presented here, uses a novel method that does not rely on edge detection but instead uses shape filters [3] to find the characteristic highlight and shadow regions of craters, after which the method matches these regions into possible crater candidates. Supervised machine learning is then applied to classify these candidates into craters and non-craters. This last step was implemented in Weka (`http://www.cs.waikato.ac.nz/ml/weka/`) using the C4.5 decision tree classifier [4] with Adaboost.

The performance of our method is evaluated on two sections of a single HRSC footprint (h0905_0000). This footprint image is about 8248×65448 pixels (or 103×818 km, or 0.9×8 degrees) in size and is centered at 6.585 degrees latitude and 311.867 degrees longitude. We split this 515 MB image into 264 (6×44) sections of 1700×1700 pixels each. To ensure the detection of craters on the boundaries of the segments, each segment includes a 200 pixels wide overlap with its neighbors. Around the center of the footprint, two neighboring sections were chosen for an initial evaluation presented in this contribution; one is used for training our algorithm and another to test it. The former was used to supply the machine learning with examples of true and false craters, while the latter was used to evaluate the crater detection performance. Craters in both sites were manually marked to provide ground truth used for quality assessment. The ground truth data contains 351 craters in the training site and 360 craters in the test site. In the training site a number (68) of true craters and features (58) which are not craters but could be mistaken as such have been marked for the purpose of training an algorithm; these examples are shown in Fig. 1. After the algorithm is trained it is applied to the same (training) site; the results are shown in Fig. 2. Fig. 3 shows the ground truth and detected craters in the second (test) site.

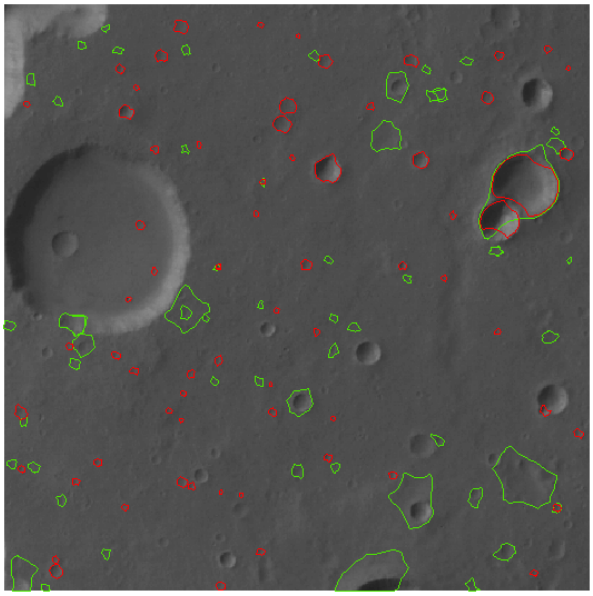

Figure 1: Training site with the true (red) and false (green) crater examples used for training the machine learning system. Best viewed on screen.

	TP	FP	FN
Training site (all)	175	10	176
Training site ($D \geq 200m$)	109	8	45
Test site (all)	198	162	36
Test site ($D \geq 200m$)	120	35	57

Table 1: Crater counts.

Quality Assessment Table 1 lists the counts and table 2 lists the quality factors in comparison with the ground truth. We use standard quality factors [5,6]: detection percentage $D = 100TP/(TP + FN)$, branching factor $B = FP/TP$, and the quality percentage $Q = 100TP/(TP + FP + FN)$, where TP is the number of true positives (detected true craters), FP is the number of false positives (detected features that are not real craters), and FN is the number of false negatives (true craters not detected by our method).

Many false negatives are craters with diameter less than 200 meters. Therefore, we show in these tables besides the results for all craters also the results for craters with diameters $\geq$ 200 meters. This is the first attempt to establish a performance limit of our method.

Discussion. As expected the results are better if only

	D	B	Q
Training site (all)	49.9%	0.06	48.5%
Training site ($D \geq 200m$)	70.8%	0.09	66.5%
Test site (all)	55%	0.18	50%
Test site ($D \geq 200m$)	67.8%	0.29	56.6%

Table 2: Quality of crater detection.

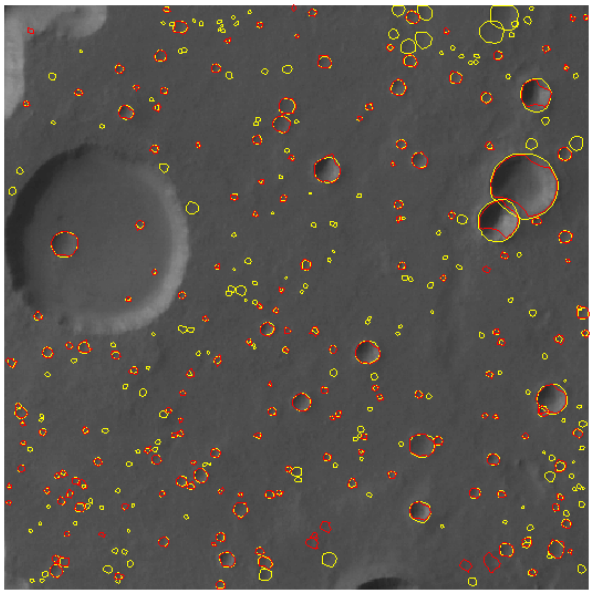

Figure 2: Training site; manually marked craters (yellow) to provide the ground truth and the craters found by our detection algorithm (red). Note that the large 7 km crater at the left of the image is outside the size range we are interested in.

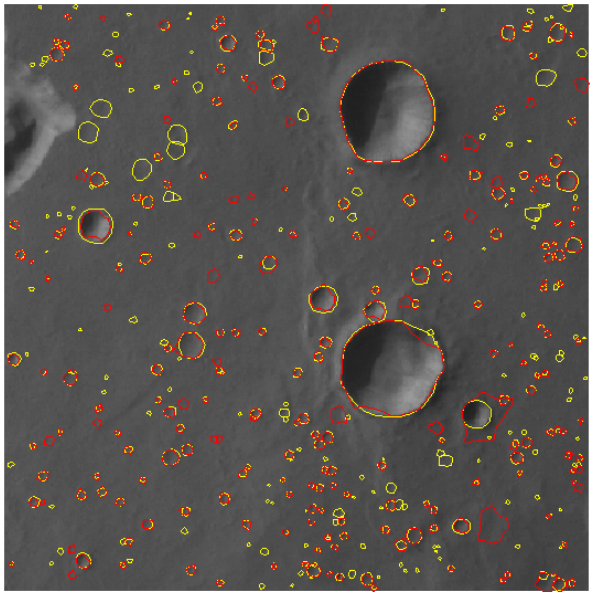

Figure 3: Test site; manually marked craters (yellow) to provide the ground truth and the craters found by our detection algorithm (red).

craters with diameters $\geq$ 200 meters are taken into account. This is because smaller craters are more difficult to detect. Interestingly, the performance on both sites is about the same indicating that the (limited set of) examples of craters and non-craters established in the training site are equally representative for both sites. Overall, the performance of our algorithm is satisfactory from feature detection point of view (it is a difficult task), but not yet quite good enough to be employed in the planetary research.

The current detection performance can be improved by using a better training set as the current set of 68 true crater and 58 false crater examples is far too limited for the large variation in appearance of the craters. We are working on constructing a training set from several sites in the aforementioned footprint image, which will be evaluated on all the sections of the footprint. This will be used to build a catalog for craters less than 5 km in diameter and will contain for each crater its location, diameter, and an estimate of its depth. A robust method for automatic detection of these smaller craters is of paramount importance as the size of the maps used and the number of craters contained is too large for manual labeling or even manual evaluation.

References

[1] Brian D. Bue and Tomasz F. Stepinski. Machine detection of martian impact craters from digital topography data. *IEEE Trans. on Geoscience and Remote Sensing*, 45(1):265–274, 2007.

[2] N. G. Barlow. Crater size-frequency distributions and a revised martian relative chronology. *Icarus*, 75(2):285–305, 1988.

[3] E. R. Urbach, N. J. Boersma, and M. H. F. Wilkinson. Vector-attribute filters. In *Mathematical Morphology: 40 Years On, Proc. Int. Symp. Math. Morphology (ISMM) 2005*, pages 95–104, Paris, 18-20 April 2005.

[4] R. Quinlan. *C4.5: Programs for Machine Learning*. Morgan Kaufmann, San Mateo, USA, 1993.

[5] J. R. Kim, J-P. Muller, S. van Gasselt, J. G. Morley, and G. Neukum. Automated crater detection, a new tool for mars cartography and chronology. *Photogramm. Eng. Remote Sens.*, 71(10):1205–1217, Oct. 2005.

[6] J.A. Shufelt. Performance evaluation and analysis of monocular building extraction from aerial imagery. *IEEE Trans. Pattern Anal. Mach. Intell.*, 21(4):311–326, Apr 1999.